J|A|C|S
ARTICLES
Published on Web 07/13/2007

Influence of Supramolecular Organization on Energy Transfer Properties in Chiral Oligo(*p*-phenylene vinylene) Porphyrin Assemblies

Freek J. M. Hoeben,[†] Martin Wolffs,[†] Jian Zhang,[‡] Steven De Feyter,*[,‡] Philippe Leclère,[†,§] Albertus P. H. J. Schenning,*[,†] and E. W. Meijer*[,†]

Contribution from the Laboratory of Macromolecular and Organic Chemistry, Eindhoven University of Technology, P.O. Box 513, 5600 MB Eindhoven, The Netherlands, the Department of Chemistry and Institute of Nanoscale Physics and Chemistry, Katholieke Universiteit Leuven, Celestijnenlaan 200F, B-3001 Leuven, Belgium, and the Service de Chimie des Matériaux Nouveaux, Université de Mons-Hainaut, B-7000 Mons, Belgium

Received April 18, 2007; E-mail: stevendefeyter@kuleuven.be; e.w.meijer@tue.nl; a.p.h.j.schenning@tue.nl

Abstract: A comparative study on oligo(*p*-phenylene vinylene) (OPV)-appended porphyrins containing all *trans*-vinylene (either hydrophilic or lipophilic) or amide linkages (lipophilic) is presented. The type of supramolecular arrangement obtained in organic solvents proves to be strongly dependent on the nature of the covalent connection. In the case of all *trans*-vinylene linkages, a J-type intermolecular packing is obtained and the assemblies are only of moderate stability. Conversely, the supramolecular structures obtained from the amide-linked system display an H-type stacking arrangement of enhanced stability and chirality as a consequence of intermolecular hydrogen bonding along the stack direction, favorably interlocking the stacked building blocks. Interestingly, the observed differences in stability and organization are qualitatively illustrated by monitoring the sequential energy transfer process in both types of assemblies. Efficient intramolecular energy transfer from the OPVs (donors) to the respective porphyrin cores is followed by energy transfer from Zn-porphyrin (donor) to free-base porphyrin (acceptor) in both systems. However, the improved intermolecular organization for the amide-linked system increases the energy transfer efficiency along the stack direction. In addition, the water-soluble (OPV)-appended porphyrin system forms highly stable assemblies in an aqueous environment. Nevertheless, the poor energy transfer efficiency along the stack direction reveals a relative lack of organization in these assemblies.

Introduction

The design of supramolecular multichromophoric arrays displaying directional energy and electron transfer is a promising strategy in the quest for organic, opto-electronic devices.[1] For this purpose, an optimal mesoscopic organization of the constituent donor and acceptor chromophores is essential for obtaining efficient energy or charge-transfer processes. Sequential energy and/or electron-transfer steps, as observed in photosynthetic systems,[2] have been studied in synthetic covalent, multichromophoric (dendritic) systems.[3] The relative ease of porphyrin synthesis and derivatization, for example, has stimulated innumerable studies dedicated to the covalent functionalization of porphyrins[4] with appended chromophores,[5] mostly for fundamental energy and electron-transfer studies. Recently, also self-assembly was accounted for in such studies.[6] Although chemists have accessibility to a rich toolbox of noncovalent interactions, in particular the synergistic interplay between multiple weak intermolecular forces is only poorly understood. Aiming for the simultaneous use of cooperative noncovalent interactions will not only allow for a fundamental understanding of the required supramolecular design principles but also be crucial to the successful implementation of functional assemblies in future applications like, e.g., artificial photosynthesis.[7]

The present paper aims for a comparative study between **1**, **2** in water[8] and similar structures (**3**, **4**) in organic solvents.

[†] Eindhoven University of Technology.
[‡] Katholieke Universiteit Leuven.
[§] Université de Mons-Hainaut.

(1) Hoeben, F. J. M.; Jonkheijm, P.; Meijer, E. W.; Schenning, A. P. H. J. *Chem. Rev.* **2005**, *105*, 1491−1546.
(2) For example, see: (a) Liu, Z.; Yan, H.; Wang, K.; Kuang, T.; Zhang, J.; Gui, L.; An, X.; Chang, W. *Nature* **2004**, *428*, 287−292. (b) Bahatyrova, S.; Frese, R. N.; Siebert, C. A.; Olsen, J. D.; van der Werf, K. O.; van Grondelle, R.; Niederman, R. A.; Bullough, P. A.; Otto, C.; Hunter, C. N. *Nature* **2004**, *430*, 1058−1062. (c) Balaban, T. S.; Holzwarth, A. R.; Schaffner, K.; Boender, G.-J.; de Groot, H. J. M. *Biochemistry* **1995**, *34*, 15259−15266.
(3) (a) Wasielewski, M. R. *Chem. Rev.* **1992**, *92*, 435−461. (b) Miller, M. A.; Lammi, R. K.; Prathapan, S.; Holten, D.; Lindsey, J. S. *J. Org. Chem.* **2000**, *65*, 6634−6649. (c) Gust, D.; Moore, T. A.; Moore, A. L. *Acc. Chem. Res.* **2001**, *34*, 40−48. (d) Imahori, H.; Guldi, D. M.; Tamaki, K.; Yoshida, Y.; Luo, C.; Sakata, Y.; Fukuzumi, S. *J. Am. Chem. Soc.* **2001**, *123*, 6617−6628. (e) Serin, J. M.; Brousmiche, D. W.; Fréchet, J. M. J. *Chem. Commun.* **2002**, 2605−2607.
(4) For example, see: (a) Balaban, T. S.; Eichhöfer, A.; Lehn, J.-M. *Eur. J. Org. Chem.* **2000**, 4047−4057. (b) Balaban, T. S.; Bhise, A. D.; Fischer, M.; Linke-Schaetzel, M.; Roussel, C.; Vanthuyne, N. *Angew. Chem., Int. Ed.* **2003**, *42*, 2140−2144. (c) Huber, V.; Katterle, M.; Lysetska, M.; Würthner, F. *Angew. Chem., Int. Ed.* **2005**, *44*, 3147−3151. (d) Balaban, T. S.; Linke-Schaetzel, M.; Bhise, A. D.; Vanthuyne, N.; Roussel, C.; Anson, C. E.; Buth, G.; Eichhöfer, A.; Foster, K.; Garab, G.; Gliemann, H.; Goddard, R.; Javorfi, T.; Powell, A. K.; Rösner, H.; Schimmel, T. *Chem.−Eur. J.* **2005**, *11*, 2267−2275. (e) Miyatake, T.; Tamiaki, H.; Holzwarth, A. R.; Schaffner, K. *Helv. Chim. Acta* **1999**, *82*, 797−810. (f) Balaban, T. S. *Acc. Chem. Res.* **2005**, *38*, 612−623.

Moreover it describes the stabilization of supramolecular assemblies by combining $\pi-\pi$ stacking interactions with intermolecular hydrogen bonding (**5**, **6**). We compare some supramolecular interactions often used and demonstrate their profound influence on the resulting self-assembly characteristics, the stability of the formed architectures, and the efficiency of the sequential energy transfer process along the stacking direction. Comparative studies of energy and/or electron-transfer efficiencies in synthetic covalent, multichromophoric (dendritic) systems have often been reported in contrast to supramolecular systems.[9]

In order to compare the different structures we first highlight the previously reported results on OPV-appended porphyrins **1** and **2** (Chart 1).[8,10] These systems are equipped with oligo(ethylene oxide) chains, thus enabling self-assembly of **1** and **2** into H-type aggregates in water. Heating these assemblies yields a chiral-to-achiral transition, although the supramolecular structures remain assembled at high temperatures due to their enormous stability. The UV/vis spectra of **1** and **2** are indicative of ground-state electronic communication between the OPVs and the porphyrin chromophores, resulting in highly modified absorption spectra with respect to reference OPV and porphyrin compounds.[5e,j] Fluorescence spectra of **1** and **2**, combined with quenching studies, display the characteristic features of efficient intramolecular energy transfer from the peripheral OPVs to both respective porphyrin cores. Furthermore, mixtures containing co-assembled **1** and **2** in water suggest cascade energy transfer from the peripheral OPVs via Zn-porphyrin to free-base porphyrin. However the energy transfer efficiency is rather low (compared to **5** and **6**, *vide infra*). This inefficiency can probably be ascribed to the relatively poor organization of these assemblies (for both features, see Table 1). The latter may be due to the presence of kinetically trapped assemblies as a result of the stability of the supramolecular structures even at high temperatures.

Chart 1. (OPVn)$_4$Porphyrins Designed to Self-Assemble into Functional Supramolecular Architectures[a]

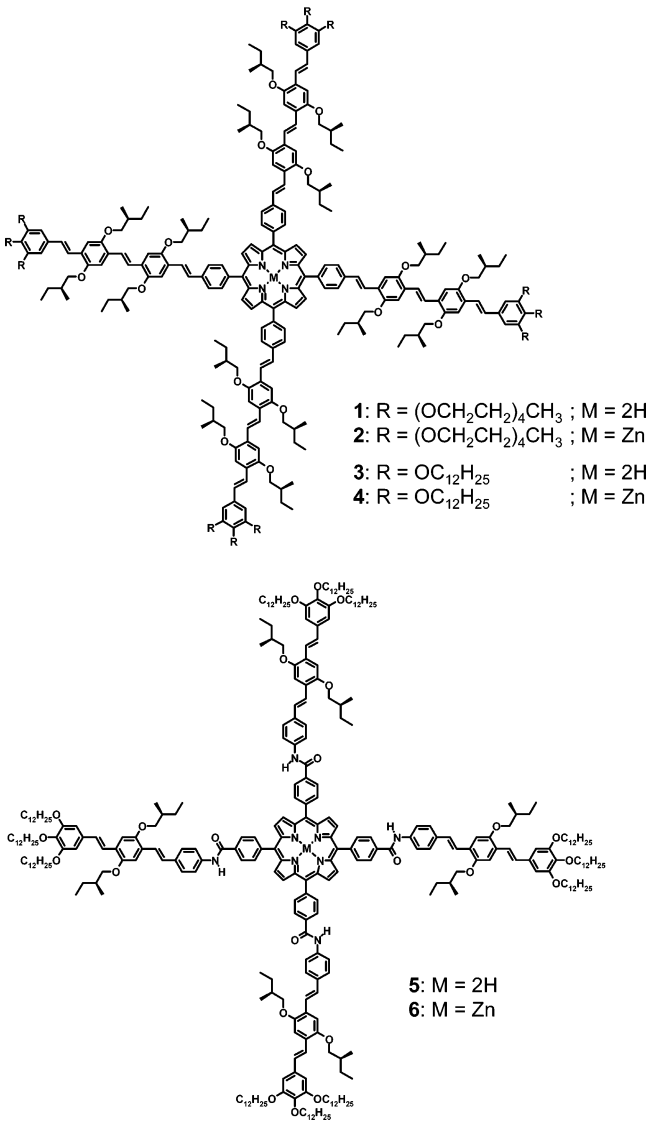

[a] (Top) Hydrophilic (OPV4)$_4$porphyrins **1** and **2** and lipophilic (OPV4)$_4$porphyrins **3** and **4** containing all-*trans* vinylene linkages. (Bottom) (OPV3)$_4$Porphyrins **5** and **6** containing amide linkages.

Results and Discussion

Self-Assembly of Apolar Analogues 3 and 4 in MCH. Apart from previously reported hydrophilic **1** and **2**,[8] their hydrophobic analogues **3** and **4** bearing aliphatic chains have been synthesized according to similar procedures (Chart 1).[10] Compounds **3** and **4** exist as dark brownish and dark greenish solids, respectively, which were fully characterized using ^{1}H NMR, ^{13}C NMR, COSY-NMR, HMQC-NMR, and IR spectroscopy, mass spectrometry, and elemental analysis.

The optical properties of **3** and **4** were investigated in chloroform and methylcyclohexane (MCH), aiming for self-

(5) For examples using various chromophores, see: (a) Vollmer, M. S.; Würthner, F.; Effenberger, F.; Emele, P.; Meyer, D. U.; Stümpfig, T.; Port, H.; Wolf, H. C. *Chem.—Eur. J.* **1998**, *4*, 260−269. (b) Holten, D.; Bocian, D. F.; Lindsey, J. S. *Acc. Chem. Res.* **2002**, *35*, 57−69. (c) Loewe, R. S.; Tomizaki, K.; Youngblood, W. J.; Bo, Z.; Lindsey, J. S. *J. Mater. Chem.* **2002**, *12*, 3438−3451. (d) Frampton, M. J.; Magennis, S. W.; Pillow, J. N. G.; Burn, P. L.; Samuel, I. D. W. *J. Mater. Chem.* **2003**, *13*, 235−242. (e) Li, B.; Li, J.; Fu, Y.; Bo, Z. *J. Am. Chem. Soc.* **2004**, *126*, 3430−3431. (f) Choi, M.-S.; Yamazaki, T.; Yamazaki, I.; Aida, T. *Angew. Chem., Int. Ed.* **2004**, *43*, 150−158. (g) Imahori, H. *Org. Biomol. Chem.* **2004**, *2*, 1425−1433. (h) Duan, X.-F.; Wang, J.-L.; Pei, J. *Org. Lett.* **2005**, *7*, 4071−4074. (i) Loiseau, F.; Campagna, S.; Hameurlaine, A.; Dehaen, W. *J. Am. Chem. Soc.* **2005**, *127*, 11352−11363. (j) Jiu, T.; Li, Y.; Gan, H.; Liu, H.; Wang, S.; Zhou, W.; Wang, C.; Li, X.; Liu, X.; Zhu, D. *Tetrahedron* **2007**, *63*, 232−240.

(6) For example, see: (a) Prokhorenko, V. I.; Holzwarth, A. R.; Müller, M. G.; Schaffner, K.; Miyatake, T.; Tamiaki, H. *J. Phys. Chem. B* **2002**, *106*, 5761−5768. (b) van der Boom, T.; Hayes, R. T.; Zhao, Y.; Bushard, P. J.; Weiss, E. A.; Wasielewski, M. R. *J. Am. Chem. Soc.* **2002**, *124*, 9582−9590. (c) de la Escosura, A.; Martinez-Diaz, M. V.; Thordarson, P.; Rowan, A. E.; Nolte, R. J. M.; Torres, T. *J. Am. Chem. Soc.* **2003**, *125*, 12300−12308. (d) Ahrens, M. J.; Sinks, L. E.; Rybtchinski, B.; Liu, W.; Jones, B. A.; Giaimo, J. M.; Gusev, A. V.; Goshe, A. J.; Tiede, D. M.; Wasielewski, M. R. *J. Am. Chem. Soc.* **2004**, *126*, 8284−8294. (e) Li, X.; Sinks, L. E.; Rybtchinski, B.; Wasielewski, M. R. *J. Am. Chem. Soc.* **2004**, *126*, 10810−10811. (f) Würthner, F.; Chen, Z.; Hoeben, F. J. M.; Osswald, P.; You, C.-C.; Jonkheijm, P.; van Herrikhuyzen, J.; Schenning, A. P. H. J.; van der Schoot, P. P. A. M.; Meijer, E. W.; Beckers, E. H. A.; Meskers, S. C. J.; Janssen, R. A. J. *J. Am. Chem. Soc.* **2004**, *126*, 10611−10618. (g) Sugiyasu, K.; Fujita, N.; Shinkai, S. *Angew. Chem., Int. Ed.* **2004**, *43*, 1229−1233. (h) Rybtchinski, B.; Sinks, L. E.; Wasielewski, M. R. *J. Am. Chem. Soc.* **2004**, *126*, 12268−12269.

(7) For some recent reviews, see: (a) Wasielewski, M. R. *J. Org. Chem.* **2006**, *71*, 5051−5066. (b) Kobuke, Y. *Eur. J. Inorg. Chem.* **2006**, *12*, 2333−2351. (c) Fukuzumi, S. *Bull. Chem. Soc. Jpn.* **2006**, *79*, 177−195. (d) Inoue, H.; Funyu, S.; Shimada, Y.; Takagi, S. *Pure Appl. Chem.* **2005**, *77*, 1019−1033. (e) Konishi, T.; Ikeda, A.; Shinkai, S. *Tetrahedron* **2005**, *61*, 4881−4899. (f) Szacilowski, K.; Macyk, W.; Drzewiecka-Matuszek, A.; Brindell, M.; Stochel, G. *Chem. Rev.* **2005**, *105*, 2647−2694. (f) Imahori, H. *Org. Biomol. Chem.* **2004**, *2*, 1425−1433. (g) Choi, M.-S.; Yamazaki, T.; Yamazaki, I.; Aida, T. *Angew. Chem., Int. Ed.* **2004**, *43*, 150−158. (h) Kobuke, Y.; Ogawa, K. *Bull. Chem. Soc. Jpn.* **2003**, *76*, 689−708.

(8) Wolffs, M.; Hoeben, F. J. M.; Beckers, E. H. A.; Schenning, A. P. H. J.; Meijer, E. W. *J. Am. Chem. Soc.* **2005**, *127*, 13484−13485.

(9) Hoeben, F. J. M.; Schenning, A. P. H. J.; Meijer, E. W. *ChemPhysChem* **2005**, *6*, 2337−2342.

(10) See the Supporting Information.

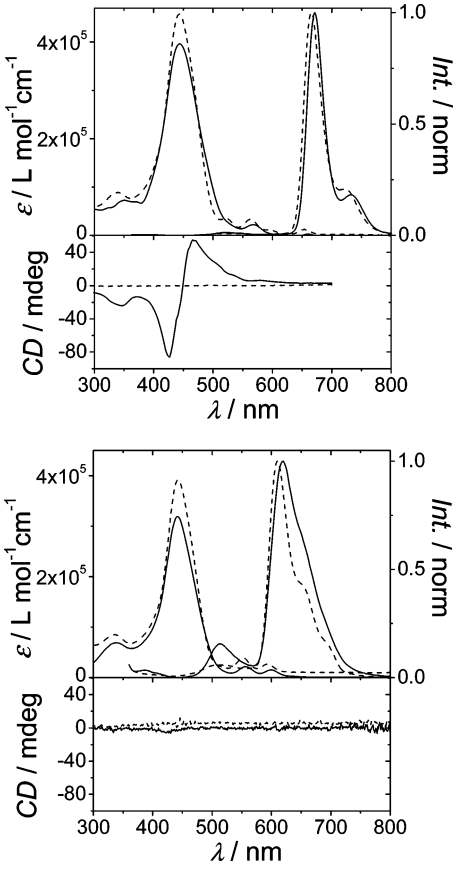

Figure 1. UV/vis, PL, and CD spectra for (top) **3** and (bottom) **4** in chloroform (dashed line) and MCH (solid line) at room temperature (10^{-5} M, $\lambda_{exc} = 346$ nm).

assembly of the molecules in the latter solvent (10^{-5} M, Figure 1).[11] In chloroform, the UV/vis spectrum of **3** displays a broad, structureless band at $\lambda_{max} = 444$ nm ($\epsilon = 4.6 \times 10^5$ L mol^{-1} cm^{-1}) accompanied by the characteristic porphyrin Q-bands[12] at common wavelengths of $\lambda = 521$, 563, 596, and 654 nm. The presence of the OPV moieties is merely revealed by their $S_2 \leftarrow S_0$ transition around $\lambda = 340$ nm. Similar to the case for **1**, the UV/vis spectrum of **3** reflects ground-state electronic communication between both chromophores. As a result, the main absorption band comprising the $\pi-\pi^*$ transition of the OPVs and the $S_2 \leftarrow S_0$ Soret band of the porphyrin is much broadened and exhibits an appreciable loss in oscillator strength.[5e,j] The fluorescence spectrum of **3** in chloroform ($\lambda_{exc} = 346$ nm, in order to excite the OPVs with maximum probability) shows characteristic porphyrin luminescence at $\lambda_{em} = 666$ nm and $\lambda_{em} = 722$ nm. OPV fluorescence is effectively quenched, indicating intramolecular energy transfer from the peripheral OPVs to the porphyrin core.[5] A quenching factor of $Q \approx 150$, determined in a comparative study on the combined fluorescence of its building blocks,[10] yields a lower limit for the energy transfer rate of $k_{ENT} = 10^{11}$ s^{-1} when a typical OPV4 lifetime of $\tau = 1.3$ ns is taken into account.[13,14] Characteristic optical changes

(11) As in the case for previously studied pure OPV assemblies, dodecane was also investigated as a non-solvent, but since **3** to **6** precipitated in this solvent the results were not reproducible.
(12) Hashimoto, T.; Choe, Y.-K.; Nakano, H.; Hirao, K. *J. Phys. Chem. A* **1999**, *103*, 1894−1904.
(13) Neuteboom, E. E.; van Hal, P. A.; Janssen, R. A. J. *Chem.—Eur. J.* **2004**, *10*, 3907−3918.
(14) Peeters, E.; Marcos, Ramos, A.; Meskers, S. C. J.; Janssen, R. A. J. *J. Chem. Phys.* **2000**, *112*, 9445−9454.

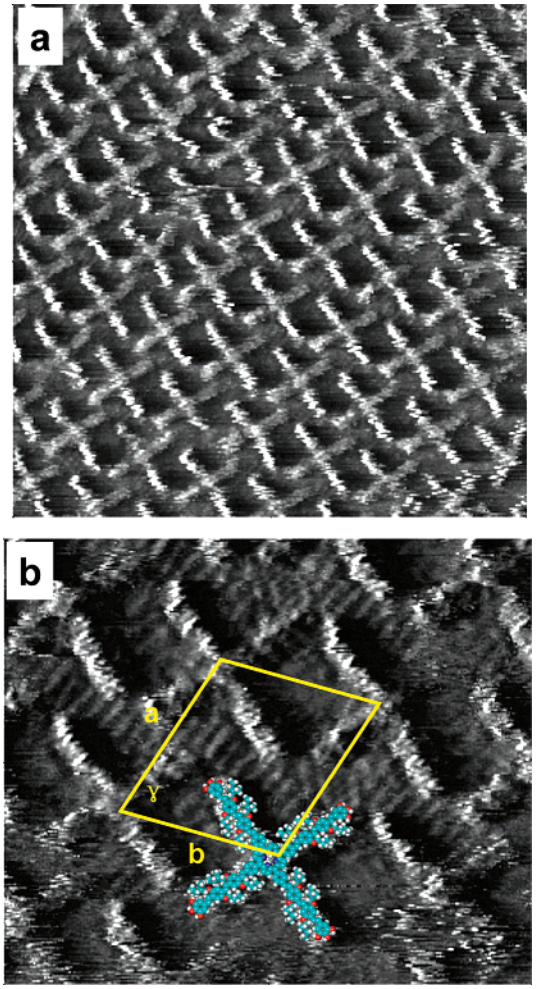

Figure 2. (a) STM image showing an ordered monolayer of **3** on HOPG, physisorbed from a 1-phenyloctane solution (1.8×10^{-5} M). Image size is 36.7 nm × 36.7 nm, $I_{set} = 0.6$ nA, $V_{set} = -0.426$ V. (b) A high-resolution STM image also revealing the adsorbed alkyl chains of **3**. A molecular model, without alkyl chains, is superimposed on the STM image. The dimensions of the unit cell are $a = 5.2$ nm, $b = 4.7$ nm, and $\gamma = 70$ °.

occur upon Zn^{2+} insertion into the porphyrin core. In chloroform, while the Soret band remains situated at $\lambda = 442$ nm ($\epsilon = 3.9 \times 10^5$ L mol^{-1} cm^{-1}), the increased symmetry of the resulting chromophore causes the $S_1 \leftarrow S_0$ transition to reduce to two Q-bands at $\lambda = 552$ and 593 nm.[12] Due to the increased energy of the $S_1 \leftarrow S_0$ transition the main emission peak is observed at $\lambda_{em} = 610$ nm with a vibrational shoulder at $\lambda_{em} = 654$ nm. OPV luminescence remains highly quenched as a result of energy transfer to the Zn-porphyrin. The 56 nm hypsochromic shift in porphyrin luminescence with regard to its free-base analogue makes Zn-porphyrin in **4** an excellent energy donor for the free-base porphyrin in **3** due to a highly favorable Förster overlap integral.[15]

Scanning tunneling microscopy (STM) measurements were performed at the liquid−solid interface by physisorbing lipophilic **3** from a 1-phenyloctane solution (1.8×10^{-5} M) onto highly oriented pyrolytic graphite (HOPG). STM images show an ordered pattern of cross-like features (Figure 2a) identified as individual molecules of **3** physisorbed parallel onto the substrate into a regular pattern. Such a regular pattern is not formed immediately but appears within a few hours after the

(15) Förster, T. *Discuss. Faraday Soc.* **1959**, *27*, 7.

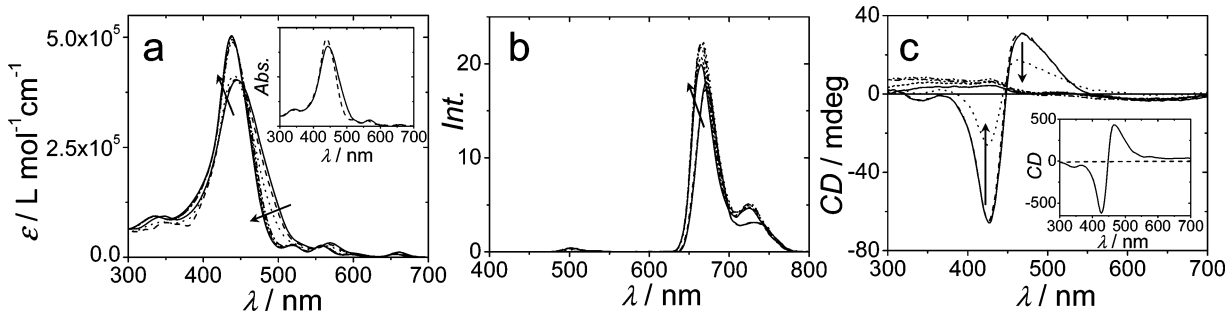

Figure 3. Temperature-dependent (a) UV/vis, (b) PL ($\lambda_{exc} = 346$ nm), and (c) CD spectra of **3** in MCH (10^{-5} M). The arrows indicate a temperature increase from 10 °C to 70 °C. The insets in (a) and (c) show the optical properties of **3** in MCH at low (10^{-7} M, dashed line) and at high (UV/vis, 10^{-4} M; CD, 6×10^{-5} M, solid line) concentrations at room temperature.

solution is applied onto the substrate and reflects relatively slow monolayer formation dynamics. When probing in more detail, also the alkyl chains of the (tridodecyloxy)wedges are observed (Figure 2b). The shape of the individual molecules and the high uniformity of the pattern indicate an all-*trans* vinylene conformation of the OPV parts.[16] As the OPV units are decorated with (*S*)-2-methylbutoxy groups, it is natural to evaluate the influence of molecular chirality on monolayer formation. The observed patterns are clearly two-dimensionally chiral, and the enantiomeric excess is reflected in the presence of one form exclusively.[17]

Upon dissolving **3** in MCH, subtle optical differences are observed. Although the position of the absorption maximum does not shift, the combined main OPV/porphyrin absorption significantly broadens and develops a shoulder which overlaps with the first Q-band absorption. Moreover, the Q-bands exhibit a bathochromic shift of approximately 5 nm. The fluorescence trace is shaped similarly as in the case of chloroform, but its main emission peak exhibits a modest 5 nm bathochromic shift to $\lambda_{em} = 671$ nm. These relatively minor effects can be assigned to self-assembly of the system by $\pi-\pi$ stacking of the conjugated backbones, since concomitantly a bisignate Cotton effect[18] emerges corresponding to the UV/vis absorption. The observed Cotton effect is positive at long wavelengths ($g = +5.8 \times 10^{-4}$ at $\lambda = 468$ nm) and negative at shorter wavelengths ($g = -8.4 \times 10^{-4}$ at $\lambda = 427$ nm) with the zero-crossing of the CD effect at $\lambda = 449$ nm. Whereas the chloroform solution lacked supramolecular chirality, $\pi-\pi$ stacking and solvophobic effects ensure the formation of functional assemblies in MCH, which remain soluble due to the surrounding apolar alkyl chain jacket. Similar UV/vis and PL changes as obtained for **3** are found for **4** when dissolved in MCH. However, the absence of a Cotton effect indicates that aggregation occurs in an achiral fashion or without preferential helicity. Concentration-dependent UV and CD measurements[10] indicate that **3** self-assembles in MCH at concentrations higher than 5×10^{-6} M at room temperature. This indicates that, despite the enlarged π-surface available for stacking interactions, relatively weak assemblies are formed with respect to pure OPV assemblies.[19] Figure 3 shows temperature-dependent UV/vis, PL ($\lambda_{exc} = 346$ nm), and CD studies on **3** in MCH (10^{-5} M). When the temperature is increased, the UV/vis spectra display a hypsochromic shift from $\lambda_{max} = 445$ to $\lambda_{max} = 438$ nm. This is combined with a narrowing of the main absorption peak which moreover gains in oscillator strength. The disassembly of the system is corroborated by the disappearance of the Cotton effect above a transition temperature of 35 °C. Upon disassembly, the emission from the sample exhibits a hypsochromic shift from $\lambda_{em} = 672$ to $\lambda_{em} = 665$ nm while remaining at a similar intensity. The combined results indicate that, at temperatures below its transition temperature, **3** self-assembles into right-handed helical J-type aggregates. As opposed to pure OPV assemblies,[19] the luminescence of **3** is not lost upon aggregation, which is a direct consequence of its J-type stacking mode.[20] At high temperature, the optical properties of **3** are similar to those in chloroform at room temperature, indicating that the chromophores are present as molecularly dissolved species. Similar temperature-dependent optical measurements on **4** in MCH[10] yield a transition temperature of 30 °C (10^{-5} M), indicating that **4** self-assembles into structures of similar stability.

The J-type stacking behavior displayed by **3** and **4** is in sharp contrast with that of compounds **1** and **2**, which assemble into H-type aggregates in water.[8] In addition, the intrinsic magnitude of the bisignate Cotton effect for **3** is enhanced with respect to **1**. Most likely, the ability of the molecules to attain their optimal organization is overruled in water as a result of the strong hydrophobicity.[21] This forces the π-conjugated surfaces together in an H-type fashion to minimize the contact with the aqueous environment and suggests that hydrophobicity is the main structural determining factor when studying π-conjugated self-assemblies in water.

In order to obtain images of the supramolecular $(OPV)_4$porphyrin assemblies in the solid state, AFM was implemented. When **3** is dropcast onto highly ordered pyrolytic graphite from MCH, fiberlike structures are observed, which are 3.5 nm in height and up to hundreds of nanometers in length. No morphological difference is observed between starting solutions containing either aggregated (Figure 4a) or disassembled (Figure 4b) chromophores. The measured height is smaller than the

(16) (a) Gesquière, A.; Jonkheijm, P.; Schenning, A. P. H. J.; Mena-Osteritz, E.; Bäuerle, P.; De Feyter, S.; De Schryver, F. C.; Meijer, E. W. *J. Mater. Chem.* **2003**, *13*, 2164−2167. (b) Miura, A.; Chen, Z.; De Feyter, S.; Zdanowska, M.; Uji-i, H.; Jonkheijm, P.; Schenning, A. P. H. J.; Meijer, E. W.; Würther, F.; De Schryver, F. C. *J. Am. Chem. Soc.* **2003**, *125*, 14968−14969. (c) Gesquière, A.; Jonkheijm, P.; Hoeben, F. J. M.; Schenning, A. P. H. J.; De Feyter, S.; De Schryver, F. C.; Meijer, E. W. *Nano Lett.* **2004**, *4*, 1175−1179. (d) Miura, A.; Jonkheijm, P.; De Feyter, S.; Schenning, A. P. H. J.; Meijer, E. W.; De Schryver, F. C. *Small* **2005**, *1*, 131−137.
(17) Ernst, K. H. *Top. Curr. Chem.* **2006**, *265*, 209−252.
(18) (a) Nakanishi, K.; Berova, N.; Woody, R. W. *Circular Dichroism*; VCH: Weinheim, 1994. (b) Berova, N.; Nakanishi, K.; Woody, R. W. *Circular Dichroism*, 2nd ed.; VCH: New York, 2000.
(19) Jonkheijm, P.; Hoeben, F. J. M.; Kleppinger, R.; van Herrikhuyzen, J.; Schenning, A. P. H. J.; Meijer, E. W. *J. Am. Chem. Soc.* **2003**, *125*, 15941−15949.
(20) Kobayashi, T., Ed. *J-Aggregates*; World Scientific: Singapore, 1996.
(21) Chandler, D. *Nature* **2005**, *437*, 640−647.

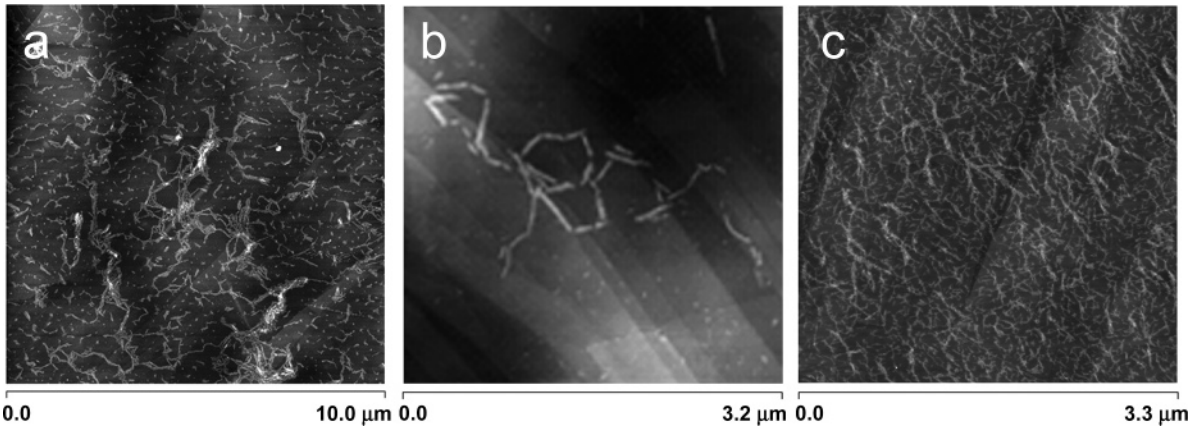

Figure 4. AFM images showing fiberlike morphologies of (a, b) **3** and (c) **5** on HOPG, dropcast from (a) 10^{-5} M, (b) 10^{-6} M, and (c) 5×10^{-6} M MCH solutions.

molecular length ($L = 5.5$ nm) implying a certain degree of tilting of the constituent chromophores inside the fibers with respect to the surface. When similar measurements are performed using either hydrophilic glass or mica surfaces, dewetting occurs and a height of 5.0 nm is found.

Sequential Energy Transfer in Mixed Assemblies of 3 and 4. The observed efficient intramolecular energy transfer from the peripheral OPVs to the porphyrin core in **3** and **4** is a prerequisite for further excitation transfer along the stacking direction. For this purpose, mixed assemblies of **3** and **4** were envisaged in which the Zn-porphyrin moiety acts as an energy donor toward the free-base porphyrin.[22] In order to avoid inner filter effects,[23] mixing experiments had to be performed at optical densities below 0.1. At these concentrations (5×10^{-7} M), however, **3** and **4** are not present as assembled species and an initial mixing experiment at 20 °C was executed for reference purposes (Figure 5, top). In order to study mixed assemblies, consecutive samples were cooled to −100 °C. At this temperature, a considerable bathochromic shift of pure **4** luminescence from $\lambda_{em} = 615$ nm to $\lambda_{em} = 654$ nm indicates chromophore aggregation. In addition, the decreasing temperature causes the shape of the fluorescence spectrum to change in favor of the 0−0 emission band, in accordance with Boltzmann's principle.[24] Excitation occurs in both cases at $\lambda_{exc} = 346$ nm, where predominantly the OPV chromophores absorb.

The reference experiment conducted at 20 °C clearly shows the increasing solution content of free-base analogue **3** (0 to 24 mol %), which emits at $\lambda_{em} = 663$ and $\lambda_{em} = 726$ nm. Performed in this way, the experiment probes energy transfer from **4** to **3** in the molecularly dissolved state, which is clearly absent since the fluorescence characteristic of **4** at $\lambda_{em} = 610$ nm remains constant. The results obtained for a similar mixing experiment at −100 °C (with acceptor addition at room temperature) are in clear contrast with the behavior at room temperature (Figure 5, bottom). Upon addition of free-base analogue **3** (0 to 26 mol %), fluorescence characteristic of **4** around $\lambda_{em} = 639$ nm is quenched to a high degree, in favor of acceptor luminescence

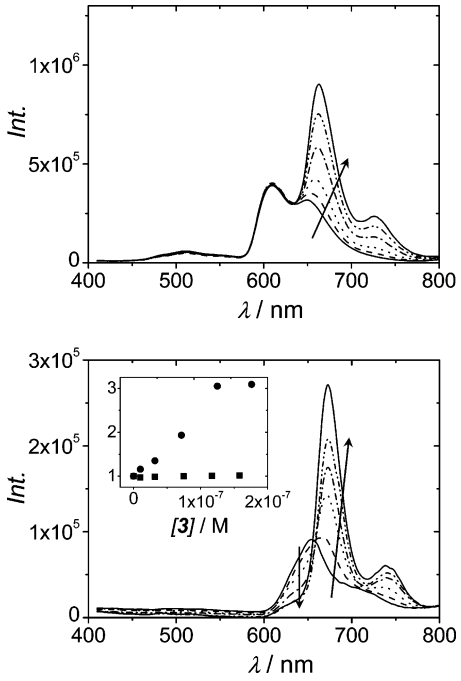

Figure 5. PL spectra for the addition of (top) 0 to 24 mol % **3** to **4** at 20 °C in MCH and (bottom) 0 to 26 mol % **3** to **4** in MCH at −100 °C. In both cases $\lambda_{exc} = 346$ nm, the concentration of **4** is fixed at 5×10^{-7} M. The inset compares donor luminescence quenching I_0/I at $\lambda_{em} = 610$ nm (■, 20 °C) and $\lambda_{em} = 630$ nm (●, −100 °C).

at $\lambda_{em} = 673$ nm and $\lambda_{em} = 739$ nm. The relative increase in acceptor fluorescence seems to exceed that observed for the disassembled state. The combined data strongly suggest a sequential energy transfer process from the peripheral OPVs via Zn-porphyrin to free-base porphyrin. However, we are at the moment not able to exclude other excitation transfer pathways, e.g., as a consequence of fast exciton diffusion among different π-stacked OPV chromophores[25] or by direct OPV (attached to Zn-porphyrin) to free-base porphyrin energy transfer. However, the poor organization of self-assembled **4** (following from the lack of supramolecular chirality) and the fast intramolecular energy transfer process to both porphyrins most likely preclude these respective supplementary pathways. In addition, it is difficult to ascertain whether the sensitized

(22) (a) Chambron, J.-C.; Heitz, V.; Sauvage, J.-P. In *The Porphyrin Handbook*; Kadish, K. M., Smith, K. M., Guilard, R., Eds.; Academic Press: London, 2000; Volume 6, pp 1−42. (b) Harvey, P. D. In *The Porphyrin Handbook*; Kadish, K. M., Smith, K. M., Guilard, R., Eds.; Academic Press: London, 2003; Volume 18, pp 64−250.

(23) (a) Alan Mode, V.; Sisson, D. H. *Anal. Chem.* **1974**, *46*, 200−203. (b) Demasa, J. N.; Crosby, G. A. *J. Phys. Chem.* **1971**, *75*, 991−1024.

(24) Atkins, P. W. *Physical Chemistry*, 6th ed.; Oxford University Press: Oxford, 1998.

(25) Herz, L. M.; Daniel, C.; Silva, C.; Hoeben, F. J. M.; Schenning, A. P. H. J.; Meijer, E. W.; Friend, R. H.; Phillips, R. T. *Phys. Rev. B* **2003**, *68*, 045203/1−045203/7.

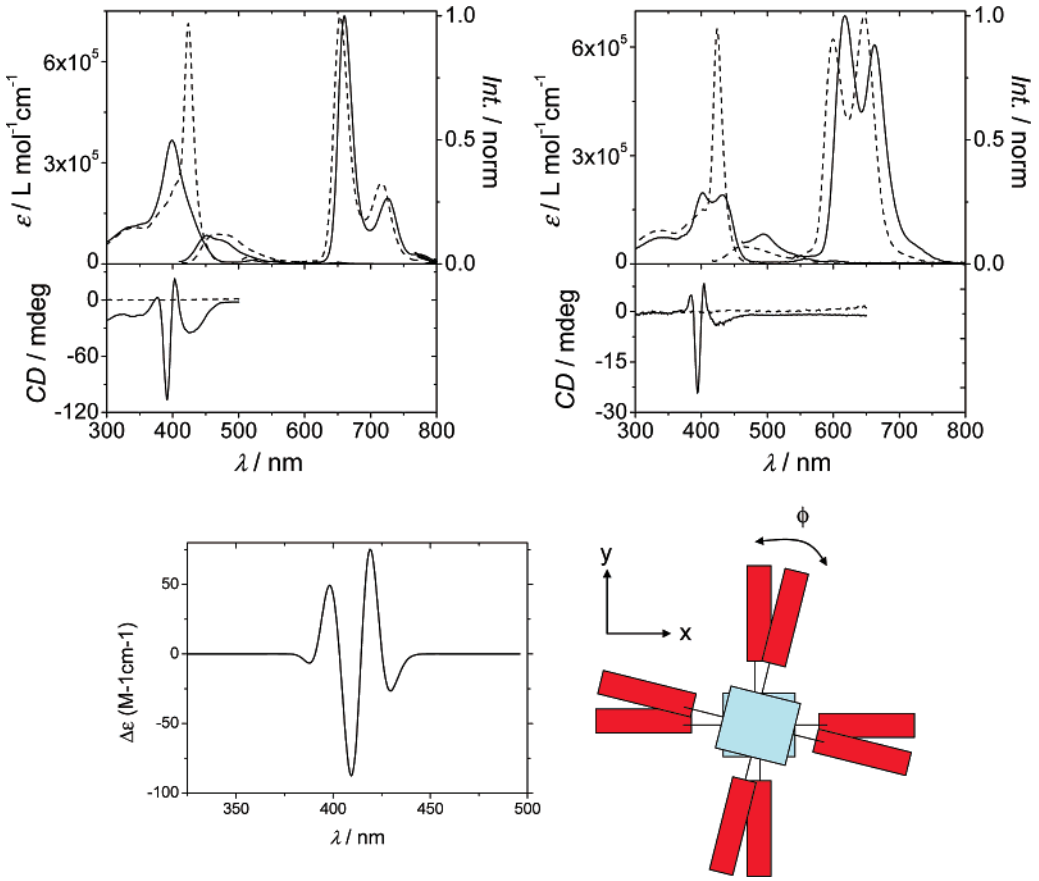

Figure 6. Top: UV/vis and normalized photoluminescence spectra ($\lambda_{exc} = 394$ nm for **5** and $\lambda_{exc} = 395$ nm for **6**) at 10^{-6} M for (left) **5** and (right) **6** and CD spectra for **5** (8.3×10^{-6} M) and **6** (9.5×10^{-6} M). Data in chloroform (dashed line) and MCH (solid line). Bottom: (left) calculated CD spectrum for **5** and (right) schematic picture (porphyrin = square, OPV = rectangle) of the supramolecular stacking arrangement of **5**.

free-base porphyrins are present as isolated energy traps or as clusters of acceptor moieties. Previously studied OPV donor/acceptor co-assemblies displayed a significant change in the vibrational ratio of sensitized acceptor luminescence, clearly indicating the clustering of acceptor molecules at higher incorporation ratio.[26] For the present system, however, no such obvious features are observed.

Hydrogen Bonding in (OPV)$_4$Porphyrin Assemblies 5 and 6 in MCH. To enhance the stability of the self-assembled lipophilic (OPV)$_4$porphyrin architectures, porphyrin derivatives **5** and **6**, connecting the peripheral OPVs to the porphyrin core via amide bonds, were synthesized. The porphyrin core was equipped with an OPV3 derivative in order to maintain the total number of phenyl rings and thus, conceivably, the overall $\pi-\pi$ stacking interactions. The carbonyl group of the amide bond was placed at the center of the system, i.e., directly attached to the porphyrin, based on previous experience with C_3-symmetrical OPV discs.[27] (OPV3)$_4$Porphyrins **5** and **6** were synthesized using standard procedures.[10] Both exist as purple solids and were fully characterized using ^{1}H NMR, ^{13}C NMR, IR spectroscopy, and mass spectrometry.

The optical properties of **5** and **6** were investigated in various solvents (Figure 6). In chloroform, both compounds are molecularly dissolved, which is concluded from their sharp, intense Soret bands at $\lambda_{max} = 424$ nm ($\epsilon = 7.1 \times 10^5$ L mol^{-1} cm^{-1} for **5** and $\epsilon = 6.5 \times 10^5$ L mol^{-1} cm^{-1} for **6**), which overlap with the $\pi-\pi^*$ transition of the OPVs. The optical transitions of the porphyrin moieties are so intense that the absorption maximum of OPV3, which is typically found at $\lambda = 400$ nm, is merely visible as a small shoulder for both molecules. In sharp contrast to **1**−**4**, the UV/vis spectra of **5** can be qualitatively reproduced by a summation of the spectra of the individual components **OPV3-NH$_2$** and 5,10,15,20-tetrakis(4-carboxyphenyl)porphyrin[10] since the amide linkage electronically isolates the chromophores. The Q-bands of both porphyrins are located at $\lambda = 516$, 552, 591, and 647 nm for **5** and at $\lambda = 548$ and 587 nm for **6**. Photoluminescence spectra of **5** and **6** in chloroform indicate that OPV fluorescence at $\lambda_{em} = 463$ nm is almost completely quenched for both systems, in favor of porphyrin luminescence. In line with previous results[8] and those presented in Figure 1 this indicates efficient intramolecular energy transfer from the OPVs to the porphyrin core, especially since the quantum yield of OPV3[14] is generally much higher than that for porphyrin derivatives. For **5**, typical porphyrin luminescence is detected at $\lambda_{em} = 654$ and $\lambda_{em} = 716$ nm with a slightly enhanced quantum yield ($\phi = 0.14$) with respect to unsubstituted tetraphenylporphyrin ($\phi = 0.11$). A comparative study for **5** and a 4:1 molar mixture of **OPV3-NH$_2$** with 5,10,15,20-tetrakis(4-carboxyphenyl)porphyrin in THF (in which **5** is molecularly dissolved) reveals that OPV fluorescence at $\lambda_{em} = 484$ nm is quenched with a factor Q_{OPV}

(26) (a) Hoeben, F. J. M.; Herz, L. M.; Daniel, C.; Jonkheijm, P.; Schenning, A. P. H. J.; Silva, C.; Meskers, S. C. J.; Beljonne, D.; Phillips, R. T.; Friend, R. H.; Meijer, E. W. *Angew. Chem., Int. Ed.* **2004**, *43*, 1976−1979. (b) Ajayaghosh, A.; Vijayakumar, C.; Praveen, V. K.; Babu, S. S.; Varghese, R. *J. Am. Chem. Soc.* **2006**, *128*, 7174−7175.
(27) van Herrikhuyzen, J.; Jonkheijm, P.; Schenning, A. P. H. J.; Meijer, E. W. *Org. Biomol. Chem.* **2006**, *4*, 1539−1545.

≈ 100 ($\lambda_{exc} = 395$ nm).[10] Combined with a typical lifetime of $\tau = 1.5$ ns for OPV3,[14] this means that the lower limit for the energy transfer rate is $k_{ENT} = 7 \times 10^{10}$ s^{-1}.[13] Fluorescence of **6** is detected at $\lambda_{em} = 600$ nm and $\lambda_{em} = 647$ nm, again indicating the large hypsochromic shift as Zn^{2+} is inserted into the porphyrin core, whereas OPV luminescence is almost completely quenched due to intramolecular energy transfer. Spin−orbit coupling with the zinc atom results in an enhanced intersystem crossing rate thereby decreasing the fluorescence quantum yield of **6** to $\phi = 0.09$.[28] The shape of its luminescence indicates that the transitions to the first and the zero-vibrational level of the ground state occur with almost equal probability, which has been observed before for Zn-porphyrins.[29]

In MCH,[11] the Soret band of both systems strongly decreases in intensity and broadens, indicative of aggregation. The absorption maximum of **5** shifts hypsochromically to $\lambda_{max} = 399$ nm ($\epsilon = 3.7 \times 10^5$ L mol^{-1} cm^{-1}) with a long shoulder extending beyond $\lambda = 450$ nm, while the Q-bands diminish in intensity and shift bathochromically to $\lambda = 520$, 556, 598, and 654 nm. This indicates the formation of H-type aggregates as a consequence of the interlocking of stacked π-surfaces by hydrogen bonding. The Soret band of **6**, however, is split into two even further diminished absorption bands at $\lambda_{max} = 402$ nm (hypsochromically shifted, $\epsilon = 2.0 \times 10^5$ L mol^{-1} cm^{-1}) and $\lambda = 432$ nm (bathochromically shifted, $\epsilon = 1.9 \times 10^5$ L mol^{-1} cm^{-1}), indicative of an oblique slipped stacking morphology for the porphyrin moiety.[30] Its Q-bands are diminished in intensity and bathochromically shifted to $\lambda = 560$ and 604 nm. Photoluminescence spectra ($\lambda_{exc} = 387$ nm, selected by comparing the UV/vis spectra of **OPV3-NH$_2$** and 5,10,15,20-tetrakis-(4-carboxyphenyl)porphyrin) show that porphyrin luminescence in **5** in MCH is highly quenched ($\phi = 0.07$) and bathochromically shifted 6 nm to $\lambda_{em} = 660$ and $\lambda_{em} = 726$ nm.[31] The luminescence of self-assembled **6** displays a larger, 18 nm bathochromic shift to $\lambda_{em} = 618$ and $\lambda_{em} = 662$ nm ($\lambda_{exc} = 401$ nm) while its fluorescence is hardly quenched ($\phi = 0.06$) as a consequence of its enhanced J-type stacking behavior. Both systems display supramolecular chirality in the assembled state as observed from their similar CD spectra, whereas no optical activity is observed in the Q-band region (nor for elevated concentrations). The intrinsic magnitude of the effect is larger for **5** ($g = +2.5 \times 10^{-4}$ at $\lambda = 403$ nm and $g = -1.3 \times 10^{-3}$ at $\lambda = 391$ nm) than for **6** ($g = +1.5 \times 10^{-4}$ at $\lambda = 404$ nm and $g = -4.5 \times 10^{-4}$ at $\lambda = 394$ nm) which stems most likely from the difference in stacking arrangement as a consequence of zinc insertion. Since the shape of the CD effect and the zero-crossing wavelengths are identical for both molecules, an alternative hypothesis suggests that **6** displays more than one stacking arrangement, of which only a potential H-type configuration is chiral. In this proposition, we believe that the latter cofacial arrangement is enforced upon the system by intermolecular hydrogen bonding (*vide infra*). Remarkably, the Cotton effects observed for both (OPV3)$_4$porphyrins do not comprise bisignate behavior, as observed for the H-type assemblies formed by **1**[8] or the J-type architectures formed by **3**, but seem to consist of two overlapping bisignate Cotton effects. To gain more insight into this specific feature we used a mathematical program[32] to calculate the CD spectrum of a supramolecular dimer consisting of two molecules of **5**. The hypsochromic shift in UV/vis indicates that the molecules are stacked on top of each other where the lateral distance is assumed to be 3.5 Å corresponding to the $\pi-\pi$ stacking interaction.[10] The measured shape of the Cotton effect could be simulated by varying the angle of rotation (φ) and the displacements in the x (dx) and y (dy) directions between two molecules of **5**, without loosing the H-type stacking arrangment. The transition-dipole moments were determined from the reference compounds **OPV4-NH$_2$** and 5,10,15,20-tetrakis(4-carboxyphenyl)porphyrin in THF and the bandwidths of the OPV $S_1 \leftarrow S_0$ transition and the Soret-band of the porphyrin were assumed to be equal.[10] In this way a spectrum can be simulated ($\varphi = 9.5°$, d$x = 3.6$ Å, d$y = 3.9$ Å) that nicely resembles the shape of the measured spectrum. This indicates that the existence of two overlapping bisignate Cotton effects (of equal sign) is a plausible interpretation for the observed behavior.

Concentration and temperature-dependent UV/vis measurements were performed on both (OPV3)$_4$porphyrins in MCH in order to establish aggregate stability.[10] The absence of any significant changes in the UV/vis spectra with decreasing concentration for self-assembled **5** and **6** indicates stability up to the point where the optical density is too low to be measured, i.e., $\sim 5 \times 10^{-8}$ M. This is an excellent improvement in supramolecular stability with respect to all *trans*-vinylene-linked **3** and **4**. Temperature-dependent UV/vis spectra of **5** in MCH at 3×10^{-7} M indicate a transition from the assembled to the dissolved phase around $\sim$85 °C (without ever becoming completely molecularly dissolved), again stressing the enormous assembly stability. An isosbestic point at $\lambda = 414$ nm confirms the presence of two coexistent species in solution. Also self-assembled **6** (3×10^{-7} M) remains stable at high temperatures indicating that, despite the change in stacking configuration, the stability of its assemblies is similar to **5**.

The proposed intermolecular hydrogen bonding via the amide functionalities was investigated using infrared spectroscopy on **5** and **6** in chloroform (5×10^{-4} M) and MCH (10^{-3} M for **5** and 7×10^{-4} M for **6**).[10] In chloroform, the absorption in the amide I region (which is mainly composed of the carbonyl stretching vibration) is detected at $\nu = 1677$ and 1674 cm^{-1} for **5** and **6**, respectively. A distinct shift to lower wavenumbers in MCH ($\nu = 1649$ and 1650 cm^{-1}, respectively) clearly indicates intermolecular hydrogen bonding in the assembled state,[33] and the narrowing of the absorption band for **5** suggests a uniform hydrogen-bonding strength. The broader signal found for **6** suggests a less uniform hydrogen-bonding strength and moreover indicates that not all chromophores are hydrogen-bonded. Combined with the UV/vis and CD spectral features, this is another indication that **6** displays more than one stacking arrangement, of which only the chiral H-type configuration is intermolecularly hydrogen bonded. On the other hand, an

(28) Doyle, R. J.; Da Campo, R.; Taylor, P. R.; Mackenzie, S. R. *J. Chem. Phys.* **2004**, *121*, 835−840.
(29) (a) Smith, K. M. *Porphyrins and Metalloporphyrins*; Elsevier: Amsterdam, 1975. (b) Prodi, A.; Teresa Indelli, M.; Kleverlaan, C. J.; Scandola, F.; Alessio, E.; Gianferrara, T.; Marzilli, L. G. *Chem.−Eur. J.* **1999**, *5*, 2668−2679.
(30) Yamaguchi, T.; Kimura, T.; Matsuda, H.; Aida, T. *Angew. Chem., Int. Ed.* **2004**, *43*, 6350−6355.
(31) It should be noted that the hypsochromic shifts for the porphyrin absorption maxima in **5** and **6** hamper selective excitation of the OPV moieties.
(32) Beckers, E. H. A.; Chen, Z.; Meskers, S. C. J.; Jonkheijm, P.; Schenning, A. P. H. J.; Li, X.-Q.; Osswald, P.; Würthner, F; Janssen, R. A. J. *J. Phys. Chem. B* **2006**, *110*, 16967−16978.
(33) (a) Schroeder, L. R.; Cooper, S. L. *J. Appl. Phys.* **1976**, *47*, 4310−4317. (b) Skrovanek, D. J.; Howe, S. E.; Painter, P. C.; Coleman, M. M. *Macromolecules* **1985**, *18*, 1676−1683.

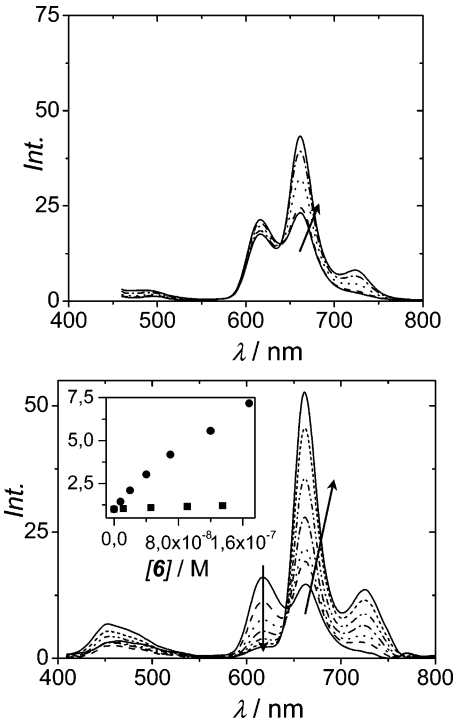

Figure 7. Photoluminescence spectra for mixtures of **5** and **6** in MCH at room temperature. The concentration of **6** is fixed at 3×10^{-7} M. (Top) Reference experiment performed by the addition of 0 to 31 mol % self-assembled **5**, $\lambda_{exc} = 433$ nm. (Bottom) Premixed samples containing 0 to 36 mol % **5**, $\lambda_{exc} = 378$ nm. The inset compares donor luminescence quenching I_0/I at $\lambda_{em} = 616$ nm of the reference (■) and the actual mixing experiment (●).

oblique slipped stacking morphology may simply prevent some carbonyl groups from participating in hydrogen bonding at all. The latter is corroborated by the temperature-dependent UV/vis experiments, which do not show any sign of disassembly at elevated temperatures, suggesting that all chromophores are hydrogen-bonded at least to some extent. At this time, we cannot clearly differentiate between these two options. These data imply that, in both systems, pre-organization via hydrogen bonding and $\pi-\pi$ stacking ensures the formation of strongly bound assemblies in MCH. Combined with the increased organization of self-assembled **5** and **6**, as expressed in their enhanced intrinsic Cotton effects when compared to **3** and **4**, this confirms that intermolecular hydrogen bonding is an excellent tool for improving stability and chirality in synthetic dye assemblies.

AFM measurements were performed on **5** by dropcasting a dilute MCH solution (3×10^{-7} M) onto HOPG. Elongated single fibers of hundreds of nanometers in length were observed with a uniform height of 2.0 nm.[10] When dropcasting a more concentrated solution (5×10^{-6} M, Figure 4c), the surface is totally covered with fibers that are highly intertwined. The height which is found for a single fiber poses a problem, since this is expected to yield the molecular length[19] (determined to be 5.6 nm for fully extended **3**). This implies a strong degree of tilting of the chromophores inside the fibers with respect to the surface.

Sequential Energy Transfer in Mixed Assemblies of 5 and 6. As a next step, energy transfer experiments using **6** and **5** as energy donor and acceptor, respectively, were conducted at donor concentrations of 3×10^{-7} M in MCH (Figure 7). The enhanced aggregate stability allows for mixing experiments to be conducted at favorable optical densities below 0.1, without having to resort to experimentally more intricate cooling conditions. However, since the $(OPV3)_4$porphyrin assemblies are never completely dissolved at high temperatures, a premixing method was implemented to obtain mixed assemblies. After mixing concentrated chloroform solutions of **5** and **6**, evaporation of the chloroform was followed by MCH addition which yielded stable solutions and reproducible results. A considerable degree of donor/acceptor mixing could be achieved by intermediate heating to 80 °C, but the eventual result was shown to be inferior to the premixing method. The high aggregate stability enables the realization of a reference experiment in MCH, in which self-assembled **5** is added to self-assembled **6** (constant at 3×10^{-7} M) at room temperature (Figure 7, top). The increase in free-base porphyrin concentration is apparent from its increased luminescence at $\lambda_{em} = 661$ nm by direct excitation. Luminescence characteristic of Zn-porphyrin at $\lambda_{em} = 617$ nm, which is now well-separated from free-base porphyrin fluorescence, is hardly affected by the acceptor addition due to the presence of separate stacks of both compounds. The premixing method indicates a completely different behavior (Figure 7, bottom). Starting with pure **6** (constant at 3×10^{-7} M in MCH), mixtures containing up to 36 mol % of free-base acceptor **5** were prepared. Excitation occurs at $\lambda_{exc} = 378$ nm in order to predominantly excite the OPV moieties. This excitation wavelength was obtained by comparing the absorption spectrum of **5** with that of aggregated **6** (directly exciting the Zn-porphyrin at $\lambda_{exc} = 433$ nm yields similar results). In the actual mixing experiment, OPV luminescence is strongly quenched due to intramolecular energy transfer to both porphyrin cores. Furthermore, eventually the luminescence of the Zn-porphyrin donor at $\lambda_{em} = 617$ nm is almost completely quenched which must imply that it further funnels the delivered excitation energy to its free-base analogue. The additional increase in free-base porphyrin luminescence at $\lambda_{em} = 661$ nm, as compared to the reference experiment, seems to confirm this hypothesis. Coinciding with the PL experiments in Figure 7, the UV/vis spectra of the mixtures of **5** and **6** confirm the addition of free-base $(OPV3)_4$porphyrin by showing a gradual increase in its typical absorption characteristics.[10] No significant differences were observed in the UV/vis data for the reference and mixing experiment of the subsequent samples.

Time-correlated single photon counting (TCPSC) was performed on pure **5** and **6** and their consecutive mixtures (premixed samples containing 0 to 36 mol % **5**, $\lambda_{exc} = 400$ nm, $\lambda_{em} = 620$ nm, 20 °C).[10] For the mixed samples, a distinct decrease in the lifetime of **6** (observed in the initial part of the spectra, $t \sim 1$ ns) is accompanied by an increase in overall lifetime with rising **5** content, due to the longer lifetime of the latter. Although the energy transfer process can be qualitatively monitored in this way, the overlapping fluorescence signals impede the measurement of any quantitative data. Also, the short time scale at which these characteristic changes occur requires more sophisticated time-resolved techniques like photoluminescence up-conversion.[26a]

Comparison of the Different Systems under Investigation. Judged from donor luminescence quenching, the energy transfer efficiency (based on acceptor incorporation) of the hydrogen-bonded donor/acceptor system **6**/**5** surpasses that of the all-*trans* vinylene linked system **4**/**3**, which in its turn is higher than that for the system **2**/**1**.[8] It is appealing to correlate the observed

differences in energy transfer efficiency to the measured differences in order parameter (*g*-value) for the respective co-assemblies, which follow a similar trend (Table 1 summarizes the properties of the $(OPV)_4$porphyrin systems studied in this paper). It has been demonstrated before that an increased degree of intermolecular order has a beneficial effect on exciton migration dynamics along stacked chromophores.[9] However, these conclusions should be handled with care, since for all three systems the degree of donor/acceptor luminescence overlap differs and the type of supramolecular packing differs. Especially the supramolecular arrangement is expected to be crucial with regard to energy-transfer characteristics.[34] Nevertheless, the novel systems **3**/**4** and **5**/**6** do seem to display an enhanced degree of cascade energy transfer, although the process is still rather inefficient when compared to, e.g., natural chlorosomal systems, their synthetic analogues,[6a] and mixed OPV assemblies previously reported.[26a]

Table 1. Comparison of the Systems under Investigation

system	**1**	**3**	**5**
electronic communication (ϵ/L mol^{-1} cm^{-1})[a]	yes (3.0×10^5)	yes (4.6×10^5)	no (7.1×10^5)
solvent for self-assembly	water	MCH	MCH
most important supramolecular interactions	$\pi-\pi$ stacking hydrophobicity	$\pi-\pi$ stacking	$\pi-\pi$ stacking H-bonding
stacking arrangement	H-type	J-type	H-type
disassembly transition temp (concentration)	no disassembly[b] (5×10^{-6} M)	35 °C (10^{-5} M)	~85 °C (3×10^{-7} M)
minimal *g*-value	-2.8×10^{-4} (10 °C)	-8.4×10^{-4} (20 °C)	-1.3×10^{-3} (20 °C)
PL quenching (I_0/I) at 25 mol % acceptor[c]	1.4 (−100 °C)	3.1 (20 °C)	5.0 (20 °C)

[a] Measured in chloroform. [b] A chiral-to-achiral transition is observed at 43 °C. [c] As a qualitative indication of the energy transfer efficiency from their donor zinc analogues.

Apart from strongly stabilizing the co-assemblies, the presence of intermolecular hydrogen bonding in MCH improves the organization of the π-stacked architectures, which consequently induces an improved energy transfer efficiency. The initial J-type configuration displayed by **3** is lost in favor of the H-type stacking arrangement of **5**, brought about by interlocking of the constituent building blocks by hydrogen bonding. Conversely, replacing the dodecyl chains of **3** with ethylene oxide chains in **1** enables self-assembly in water, where strong hydrophobic forces impose an H-type stacking mode on the system. Tentatively, this unexpected configuration is not the most stable arrangement for the system, as reflected in its diminished degree of order and cascade energy transfer efficiency. Moreover, the lack of reversible assembly demands additional optimized preparation techniques, as shown before in related literature studies.[35] This imposes the question whether simply replacing the solubilizing dodecyl chains for ethylene oxide ones is a good strategy for obtaining well-defined supramolecular architectures in water. These data clearly illustrate the strength of a supramolecular approach where various interactions can be simultaneously employed to guide self-assembly into desired functional nanostructures. However, it also demonstrates the delicate interplay of and the relative lack of control over these interactions resulting in, e.g., non-reversibility for **1** and **5**, and their zinc-incorporated analogues.

Conclusions

From this report, it becomes apparent that the successful design of supramolecular architectures displaying efficient and directional energy transfer will rely on an intricate combination of noncovalent interactions. These combined interactions will have to be carefully optimized in order to achieve the desired degree of organization and the guarantee that subsequent excitation transfer steps occur with high efficiency. In this contribution, we intended the implementation of intermolecular hydrogen bonding to significantly increase the intermolecular energy flux along the stacking direction. The desired assembly stabilization and organization clearly occurred; however, only a modest increase in energy transfer efficiency was observed. In addition, upon going from an apolar environment to water, the stacking mode of identical chromophores (the solubilizing chains put aside) unpredictably changed from a J- to an H-type arrangement. Concomitantly, the desired, internal organization of the π-stacked architectures was partly lost which was reflected in a further diminished energy transfer efficiency through the assemblies. This indicates that the strategy for solubilizing π-conjugated systems in water by attaching oligo(ethylene oxide) wedges needs reassessment in order to obtain improved assembly characteristics.

On a more general level this implies that, even though the knowledge of successfully implementing noncovalent interactions has not ceased to grow, especially their synergistic interplay will depend on the development of a comprehensible set of design rules. The synthesis of the covalent π-conjugated donor/acceptor systems presented here, their subsequent chiral self-assembly, and sequential energy transfer processes have effectively illustrated the significant differences in their resulting supramolecular architectures. Although a relative lack of control over supramolecular structure is evident (especially upon going to water), the different supramolecular design strategies used here serve as a starting point for future progress.

Acknowledgment. The authors in Eindhoven thank the Council for Chemical Sciences of The Netherlands Organization for Scientific Research (NWO-CW). We thank Dr. Pascal Jonkheijm for additional AFM measurements, Dr. Stefan C. J. Meskers for help with modeling, and Prof. René A. J. Janssen for stimulating discussions. The authors in Leuven thank the Federal Science Policy through IUAP-V-03. Support from the Fund for Scientific Research-Flanders (FWO) and K.U. Leuven is also acknowledged. Ph.L. is Chercheur Qualifié of the Fonds National de la Recherche Scientifique (FNRS-Belgium).

Supporting Information Available: Synthetic procedures and full characterization of $(OPVn)_4$porphyrins **3** to **6**, precursors **OPV3-NO$_2$** and **OPV3-NH$_2$**, and reference compound **OPV4-aldehyde**. Characteristics of the previously reported $(OPV4)_4$porphyrins **1** and **2** (Figure S1). Comparison of optical character-

(34) Beckers, E. H. A.; Meskers, S. C. J.; Schenning, A. P. H. J.; Chen, Z.; Würthner, F.; Marsal, P.; Beljonne, D.; Cornil, J.; Janssen, R. A. J. *J. Am. Chem. Soc.* **2006**, *128*, 649−657.
(35) (a) Brunsveld, L.; Lohmeijer, B. G. G.; Vekemans, J. A. J. M.; Meijer, E. W. *Chem. Commun.* **2000**, 2305−2306. (b) Hoeben, F. J. M.; Shklyarevskiy, I. O.; Pouderoijen, M. J.; Engelkamp, H.; Schenning, A. P. H. J.; Christianen, P. C. M.; Maan, J. C.; Meijer, E. W. *Angew. Chem., Int. Ed.* **2006**, *45*, 1232−236.

istics of **3** with its building blocks (Figure S2); concentration-dependent UV/vis and CD spectra of **3** in MCH (Figure S3); temperature-dependent UV/vis spectra of **4** in MCH (Figure S4); comparison of optical characteristics of **5** with its building blocks (Figure S5); temperature-dependent UV/vis spectra on **5** and **6** (Figure S6); additional AFM measurements on **5** (Figure S7); UV/vis spectra for mixtures of **5** and **6** in MCH (Figure S8); TCSPC data for **5**, **6**, and mixtures (Figure S9); model of a supramolecular dimer of **5** and the corresponding calculated UV/vis and CD spectra (Figure S10); and FT-IR measurements of **5** and **6** in chloroform and MCH including a model for the hydrogen bonds in **5** (Figure S11).

JA072548C